

## Intrinsic satellites in the $L_{23}VV$ Auger spectra of $3d$ transition metals

C. P. Lund and S. M. Thurgate

*School of Mathematical and Physical Sciences, Murdoch University, Murdoch, WA 6150, Australia*

A. B. Wedding

*School of Applied Physics, University of South Australia, The Levels SA 5095, Australia*

(Received 17 September 1993)

Auger photoelectron coincidence spectroscopy (APECS) confirms that a substantial part of the low-energy tail of the  $L_{23}VV$  Auger lines of the  $3d$  transition metals is due to intrinsic initial- and final-state shake-up/shake-off processes and not just secondary losses. Data were collected for the  $L_{23}VV$  Auger lines of pure Cu, Co, and Ni. APECS enables a direct experimental measurement of the initial-state shake-up/shake-off satellites in solid-state Auger spectroscopy. The importance of these effects in Auger spectroscopy as a qualitative and quantitative surface-analysis technique is discussed.

### I. INTRODUCTION

Auger-electron spectroscopy (AES) is widely used as a means of quantitative surface analysis. The Auger decay process is complex, involving at least three electrons, and often there are a number of competing decay channels open which result in complex spectral features. Furthermore the emitted electron can undergo a number of inelastic loss processes on the way out of the solid. Each Auger peak in the spectrum is accompanied by an increase in the background intensity on the low-energy side that extends over a range of several hundred electron volts. This tail originates from electrons, excited at various depths, which have lost energy either during transport out of the solid (extrinsic loss) or due to an intrinsic process.

Early theoretical calculations<sup>1-3</sup> pointed out that due to the electrostatic screening of the core hole created in the ionization process, any peak in a solid is always expected to be accompanied by electrons with lower energy. These *intrinsic* electrons form a tail on the low-energy side of a peak which extends 2-3 plasmon excitations below the main peak.<sup>4,5</sup> They are part of the primary excitation spectrum and should not be confused with *extrinsic* electrons, which are due to the transport of excited electrons in the solid. Although the theoretical understanding of intrinsic electron excitation is presently not at a point where exact quantitative prediction over a wide energy range can be given, it is well established<sup>1-5</sup> that qualitatively any primary peak, after removal of the extrinsic background electrons, must be asymmetric.

The first serious problem in electron spectroscopy is to isolate that part of a measured spectrum which consists of inelastically scattered electrons and thus determine the electron energy distribution at the point of excitation in the solid. A correct procedure is necessary for peak-shape analysis, for the separation of close-lying peaks, and for peak area determination. The problem has been discussed by several authors, and a number of methods have been suggested.<sup>6</sup>

Tougaard<sup>6</sup> has produced a number of expressions that

show the dependence of the inelastic background on the energy-loss function of the material in which the atom is buried and the depth distribution of the emitters. The energy-loss function depends on the details of a variety of energy-loss processes that can take energy from an escaping electron. There are a number of calculations of this function for a range of materials.<sup>7</sup> Tougaard<sup>6</sup> proposed a "universal" loss curve that describes the broad features of the energy-loss function for a range of materials. This is a function of two element dependent constants. Tougaard<sup>6</sup> illustrated the use of this function in removing the extrinsic loss from x-ray photoemission spectroscopy (XPS) curves.

Auger photoelectron coincidence spectroscopy (APECS) has the ability to reduce the complexity of spectra,<sup>8</sup> and enables the measurement of the same quantity at two different inelastic mean free paths (IMFP's). We have used this to study the nature of the intrinsic and extrinsic contributions to the low-energy tail of the  $L_{23}VV$  Auger lines of some of the  $3d$  transition metals. The coincidence results reveal a significant component of the background that is not either extrinsic loss nor a component that is in coincidence with any major excitation at higher energy.

### II. EXPERIMENT

APECS measurements have been carried out on a number of systems in  $3d$  metals using our previously described system.<sup>8</sup> Briefly it consists of two  $127^\circ$  cylindrical analyzers that have been constructed with a view to having very good timing resolution, together with appropriate coincidence electronics. These are housed in a conventional UHV chamber with a base pressure of  $2 \times 10^{-10}$  Torr. The samples included Cu and Co prepared from foils, and Ni prepared from a single crystal. They were repeatedly cleaned by being ion bombarded with 1-KeV  $\text{Ar}^+$  ions and heating every 12 h. No evidence of oxygen or carbon contamination was found after 12 h of data collection.

APECS can be used to produce two estimates of emis-

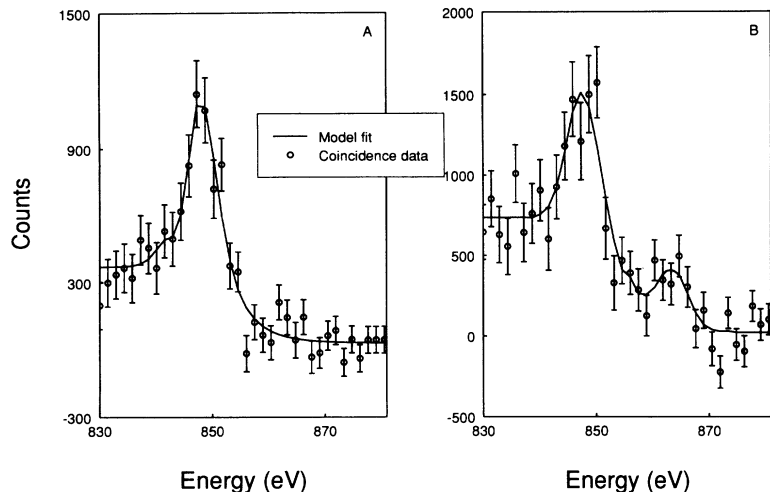


FIG. 1.  $L_{23}VV$  Auger spectrum of Ni in coincidence with (a)  $2p_{3/2}$  and (b)  $2p_{1/2}$  photoelectrons. The solid line through the raw data is a model fit using the sum of one or more Gaussians to the curves.

sion lines at different IMFP's from the same set of data, a coincidence spectrum and a singles spectrum, simultaneously. The comparison between these two will be free from any distortion due to instrumental changes. In our coincidence experiment this is done by setting one analyzer on the maximum of the photoelectron peak while the other analyzer scans the Auger line over the required energy range. We collected spectra that show the difference in time between electrons arriving in each analyzer for each setting of the scanning analyzer. These time-to-amplitude spectra were then analyzed by summing the counts in a time window that corresponds to the difference in time between electrons from the same event being detected in each analyzer. This gave the coincidence spectrum. The singles spectrum was obtained by summing all counts, regardless of the time at which the electrons were detected. This provided a means of obtaining both a singles spectrum and a coincidence spectrum from the same data set. Each coincidence spectrum took on average four weeks to acquire.

### III. RESULTS AND DISCUSSION

The Ni  $L_{23}VV$  spectrum in coincidence with  $2p_{3/2}$  and  $2p_{1/2}$  emissions are shown in Fig. 1. The Cu and Co data have been published elsewhere.<sup>10</sup> The component coincidence data were fitted with a model spectrum which is the sum of one or more Gaussians, before combining to form the full coincidence spectrum. As demonstrated by Haak, Sawatsky, and Thomas,<sup>11</sup> the  $L_3VV$  has a substantial component from the  $L_2L_3V-L_3VV$  process due to a Coster-Kronig spectator valence-band hole. To determine the full  $L_{23}VV$  coincidence spectrum it was necessary to add the  $L_{23}VV$  spectrum in coincidence with the  $2p_{3/2}$  to the  $L_{23}VV$  in coincidence with the  $2p_{1/2}$  in a ratio of 2:1. This is the ratio of the  $2p_{3/2}$  to  $2p_{1/2}$  emission. These singles and full coincidence spectra for Co, Ni, and Cu are presented in Fig. 2. We expect that there could be differences between the singles and full coincidence spectra for the following reasons.

(i) Some intensity in the singles spectrum may not

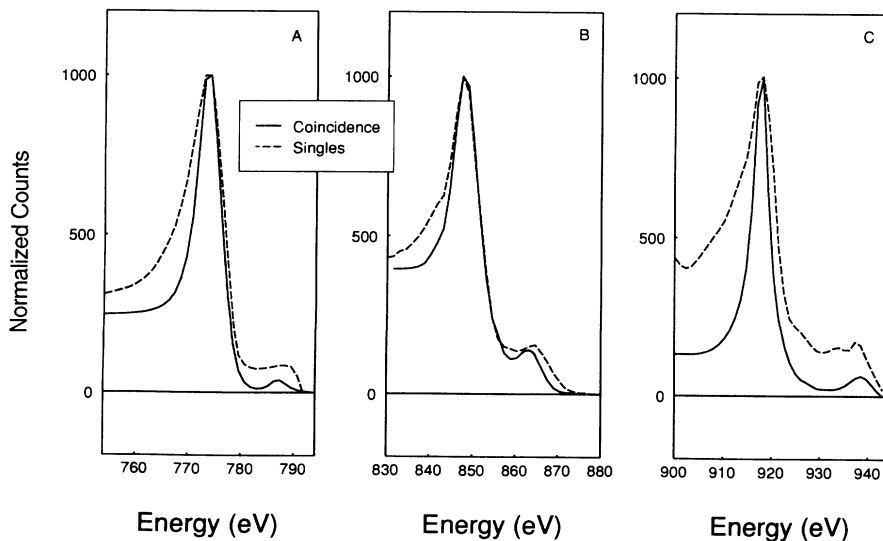


FIG. 2. Single  $L_{23}VV$  Auger spectra of (a) Co, (b) Ni and (c) Cu compared with the sum of the  $2p_{1/2}$  and  $2p_{3/2}$  coincidence spectra. The solid line represents the least-squares "best fit" to the coincidence data with the sum of several Gaussians.

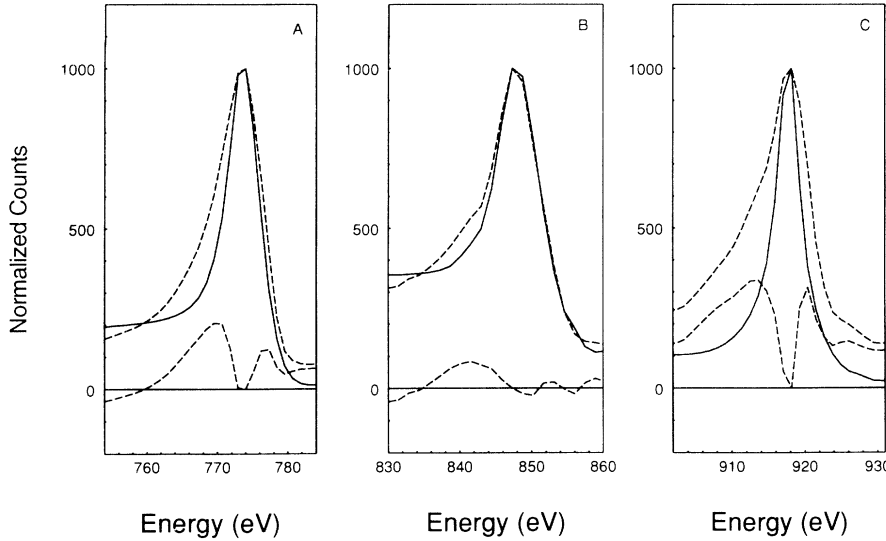


FIG. 3.  $L_3VV$  singles, coincidence, and difference spectra for (a) Co, (b) Ni, and (c) Cu after subtraction of the Tougaard (Ref. 6) "universal" loss function.

occur in coincidence with the other line under the other analyzer.

(ii) The escape depth of electrons is shorter in coincidence measurements than in the singles. This is because both electrons must be detected. The effective inelastic mean free paths (IMFP) can be calculated from<sup>8</sup>

$$\frac{1}{\lambda_{\text{eff}}} = \frac{1}{\lambda_A} + \frac{1}{\lambda_P}, \quad (1)$$

where  $\lambda_A$  is the IMFP of the Auger electron and  $\lambda_P$  is the IMFP of the photoelectron.

Tougaard<sup>6</sup> has proposed a "universal" loss curve that describes the broad features of the energy-loss function for a range of materials of the form:

$$K(E, T) \cong \frac{1}{\lambda_0} \sqrt{(E_0/E)} \frac{BT}{(C+T)^2}, \quad (2)$$

where  $\lambda_0 = \lambda(E_0)$  and  $B$  and  $C$  are element-dependent constants.  $K(E, T)$  is the differential inelastic-electron-scattering cross section, i.e., the probability that an electron of energy  $E$  shall lose energy  $T$  per unit energy loss and per unit path length traveled in the solid.

Tougaard<sup>6</sup> has also shown that one may find the primary excitation spectrum  $F(E)$  at a point of excitation of the solid by using the equation

$$F(E) = j(E) - \lambda \int_E^\infty K(E' - E) j(E') dE', \quad (3)$$

where  $j(E)$  is the flux of emitted electrons as measured experimentally.

We used Tougaard's formalism with the IMFP values of Tanuma, Powell, and Penn<sup>12</sup> to account for the extrinsic loss in each of the singles and coincidence spectra. After background subtraction, these Tougaard background subtracted results are shown in Fig. 3 together with the difference between the singles and coincidence. After background subtraction we consistently found that (i) although the tails were brought closer together on the low-energy side, they were not brought to zero; and (ii) there was distinct structure and intensity in the difference between the coincidence spectra and the singles spectra.

There are three possible explanations of these data. These are the following.

(1). The energy-loss function for the surface region is quite different than for the bulk. The coincidence data has a shorter IMFP, so the loss function suitable for this region may be quite different from that of the bulk, which makes a larger contribution to the singles spectra.

(2). There is a contribution from another core-level component in the  $L_{23}VV$  spectra that is present in the singles spectra but absent in coincidence.

(3). The difference is due to an intrinsic shake-up/shake-off process in the initial and/or final states.

The first of these can be ruled out by comparison of the photoelectron spectra collected in coincidence with the singles spectra shown in Fig. 4. If the process generating the difference in the spectra was due to change between the surface and bulk loss functions, then the effect should be seen in the photoelectron lines as well. A similar difference in IMFP's exists for the photoelectron data as for the Auger data. As can be seen from Fig. 4, there is no evidence of a significant background difference in the coincidence spectra compared to the singles spectra.

The second explanation also appears unlikely. These spectra were collected with Mg  $K\alpha$  radiation and therefore the only other level excited by this radiation that could decay into the  $2p_{3/2}$  level (besides the  $2p_{1/2}$ , which we have accounted for) is the  $2s$ . There is not enough intensity in the  $2s$ , however, to account for the magnitude of the missing background, though it may make some small contribution via decay chains such as  $L_1 \rightarrow L_2V \rightarrow L_3VV \rightarrow VVVV$ .

We conclude that the intensity is likely to be due to intrinsic shake-up/shake-off processes. A number of recent studies<sup>13-15</sup> of the  $L_2M_{45}M_{45}$  and  $L_3M_{45}M_{45}$  spectra of Cu, Zn, and Ni have shown the presence of significant shake-up/shake-off components on the low-energy side of these lines. Previous coincidence measurements<sup>16</sup> of the  $L_2M_{45}M_{45}$  spectrum of Cu in coincidence with the  $2p_{1/2}$  photoelectron have shown that the  $L_2M_{45}M_{45}$  satellite is due in part to a shake-up/shake-off process  $L_2M_{45}M_{45}M_{45}$ , and part to the Coster-Kronig process

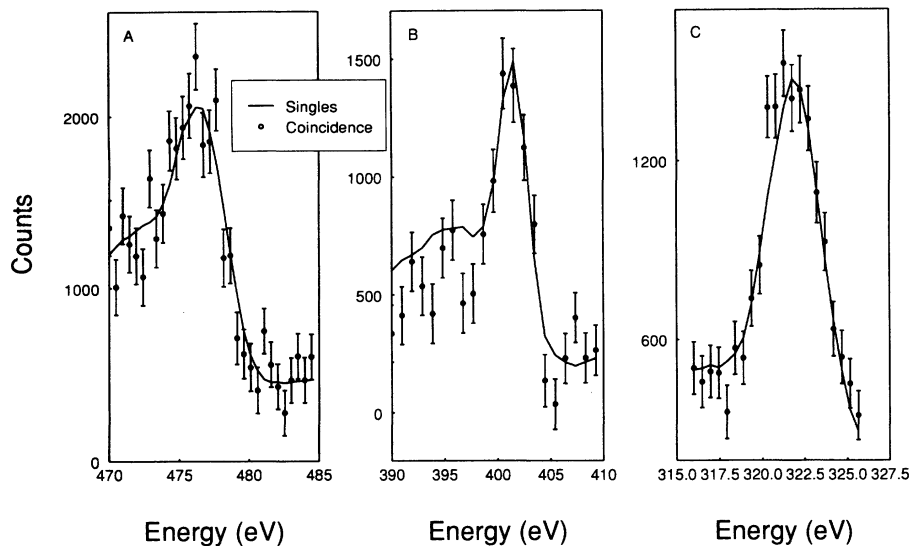


FIG. 4.  $2p_{3/2}$  photoelectron spectra for (a) Co, (b) Ni, and (c) Cu in coincidence with the  $L_3VV$  Auger line.

$L_1L_2M_{45}$  producing a vacancy spectator for the  $L_2M_{45}M_{45}$  process.

The mechanisms that lead to states with three and four  $3d$  vacancies following  $L$ -shell photoionization of metallic Ni have been investigated by Whitfield *et al.*<sup>14</sup> using synchrotron radiation. Four channels leading to the four- $3d$ -hole final state and three channels leading to the three- $3d$ -hole state, including Auger cascades and shake processes, were clearly identified and their respective roles established, convincingly verifying a model proposed by Martensson, Nyholm, and Johansson.<sup>15</sup> If primary ionization is accomplished with x-ray photons whose energy exceeds the  $L_1$  binding energy of the atom, the three-hole final state  $L_3M_{45}^3$  can arise through the channels<sup>15</sup>

Coster- Kronig

- (i)  $L_1 \rightarrow L_3M_{45} \rightarrow M_{45}M_{45}M_{45}$ ,
- (ii)  $L_2 \rightarrow L_3M_{45} \rightarrow M_{45}M_{45}M_{45}$ ,

Shake-up/shake-off

- (iii)  $L_3M_{45} \rightarrow M_{45}M_{45}M_{45}$ .

The four-hole final state  $L_3M_{45}^4$  can be produced through four different channels:<sup>15</sup>

Coster- Kronig

- (iv)  $L_1 \rightarrow L_2M_{45} \rightarrow L_3M_{45}M_{45} \rightarrow M_{45}M_{45}M_{45}M_{45}$ ,

Shake-up/ shake-off

- (v)  $L_1M_{45} \rightarrow L_3M_{45}M_{45} \rightarrow M_{45}M_{45}M_{45}M_{45}$ ,
- (vi)  $L_2M_{45} \rightarrow L_3M_{45}M_{45} \rightarrow M_{45}M_{45}M_{45}M_{45}$ .
- (vii)  $L_3M_{45}M_{45} \rightarrow M_{45}M_{45}M_{45}M_{45}$ .

These processes are illustrated schematically in Fig. 5. Of these processes none will appear in coincidence with the  $2p_{3/2}$  photoelectron peak, and only process (ii) will appear in coincidence with the  $2p_{1/2}$  photoelectron peak.

As already discussed the Coster-Kronig process,  $L_2 \rightarrow L_3M_{45} \rightarrow M_{45}M_{45}M_{45}$  will appear under the  $L_3VV$  line in coincidence with the  $2p_{1/2}$  photoelectron. Therefore we know the energy of the three-hole state from the  $2p_{1/2}$  coincidence measurements. The three-hole energy is close to the main  $L_3M_{45}^2$  peak while the difference peak in Ni [Fig. 3(b)] appears at about 7 eV below the main peak. This is the same position as the four-hole satellite in the Ni data of Martensson, Nyholm, and Johansson.<sup>15</sup> Therefore we conclude that it is likely to be a four-hole final state as proposed by Martensson, Nyholm, and Johansson.<sup>15</sup>

As the photoelectron analyzer is tuned to the main part of the peak, the coincidence spectra will not contain any component where an initial-state shake has occurred. These photoelectrons will not be energy correlated and will therefore not be detected in coincidence with the main photoelectron peak. This can be seen in the  $2p_{3/2}$  photoelectron coincidence spectra of Ni in Fig. 4, where no intensity is evident in the shake satellite in coincidence with the main part of the  $L_3VV$  Auger peak. We can therefore obtain a direct experimental measurement of the satellite arising from the intrinsic four-hole state by taking the difference between the Tougaard subtracted singles and coincidence spectra, as shown in Fig. 3.

The intensity left under the Tougaard corrected coincidence peak in Fig. 3 is likely to be due to final state shake-up/shake-off. In a final-state shake process energy is transferred to valence-band electrons as they attempt to screen the changes in core-level configurations during the emission of the Auger electron, following the initial ionization. Spectra taken in coincidence will still contain a contribution from intrinsic final-state shake processes as the initial photoelectron is unaffected by the final state shake-up/shake-off and is therefore still energy correlated. Jensen *et al.*<sup>17</sup> have found a similar effect in the APECS  $L_{23}VV$  spectrum of Al. They concluded that much of the large intensity left under their coincidence spectra was due to an intrinsic process and not due to secondary electron scattering.

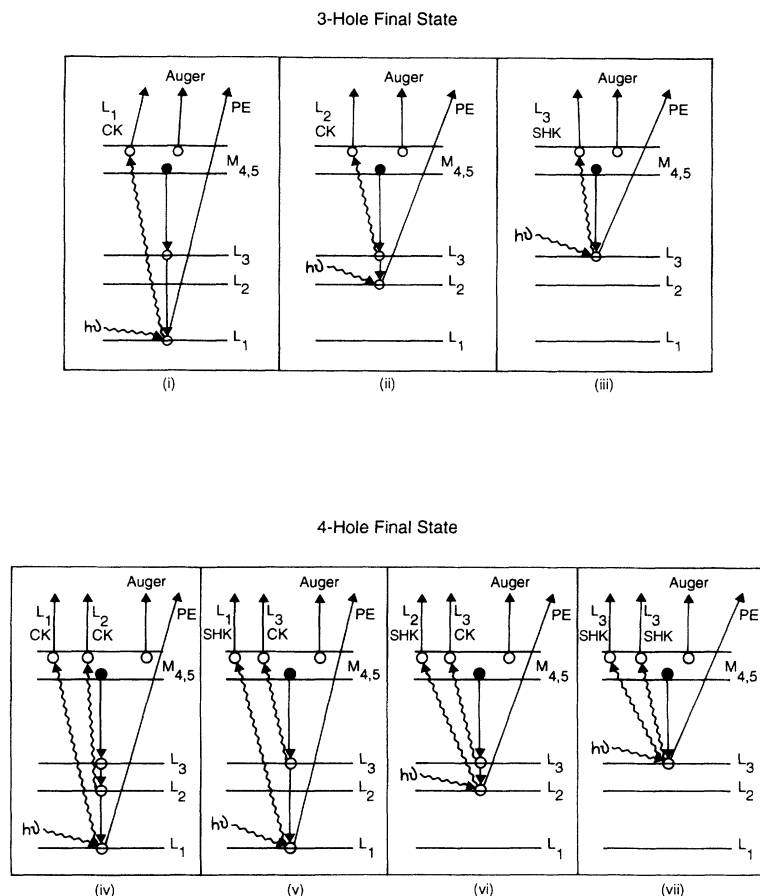


FIG. 5. Schematic representation of the channels that lead from Ni  $L$ -shell ionization to a state with three or four  $3d$  holes as proposed by Martensson, Nyholm, and Johansson (Ref. 15) and Whitfield *et al.* (Ref. 14). Only active electrons are shown, and direct processes are indicated, exchange transactions being omitted. Wavy lines indicate photons, real or virtual. Valence electron events are labeled as they occur from left to right. PE, photoelectron; CK, Coster-Kronig electron; and SHK, shake-up/shake-off electron.

In view of this discussion, we conclude that the singles spectra (in Fig. 2), are made up of four contributions as shown schematically in Fig. 6: (i) the natural (or main) line shape made up of contributions from the  $L_2$  and  $L_3$  levels; (ii) the extrinsic secondary loss background due to transport out of the solid; (iii) Intrinsic *initial-state* (shake-up/shake-off) contributions; and (iv) Intrinsic *final-state* (shake-up/shake off) contributions. The coincidence spectrum (in Fig. 2) will contain only three contributions, the true Auger line shape, an extrinsic second-

dary loss contribution (less than the singles due to a lower IMFP), and the final-state (shake-up/shake-off) contribution.

These results have important implications for the use of Auger spectroscopy as both a qualitative, as in Auger line-shape analysis (ALA) and quantitative surface analysis (AES) technique. The shake-up/shake-off satellites, both initial and final state are broad and relatively featureless and the determined intensity will, therefore, depend strongly on the background subtraction. Considering the large width of these satellites it is clear that their integrated intensity may be significant even at reasonable distances from the main peak. From their analysis Martensson, Nyholm, and Johansson<sup>15</sup> have calculated that the  $L_3M_{45}^2 \rightarrow M_{45}^4$  satellite in Ni will have an intensity of the order of 20–30% relative to the main peak  $L_3M_{45}^2$  Auger lines. Our results have shown both the intensity and the position of this satellite to vary significantly between elements. Carlson<sup>18</sup> has commented that Auger lines and their satellites can stretch over a range of 169 eV. Therefore the area under the tails of the Auger peaks should be added for quite some distance below the main line. As the shake-up/shake-off satellites vary from element to element, it is difficult however to know how far below the main peak to consider for both background subtraction and peak area integration without a knowledge of the satellites. In ALA the shape, energy position, and intensity of the shake-up/shake-off satellite needs to be accurately known before a correct in-

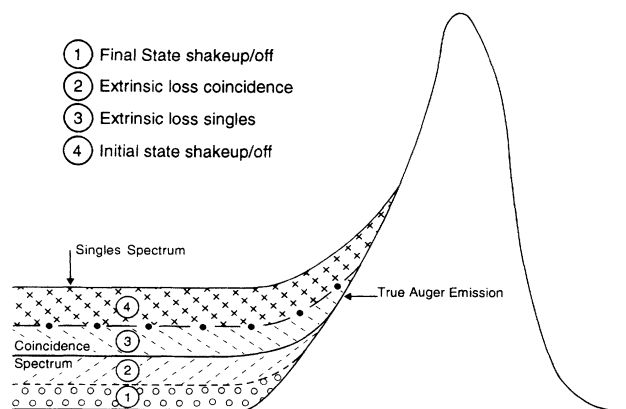


FIG. 6. Schematic diagram of the proposed contributions to the singles and coincidence Auger spectra as discussed in the text.

terpretation can be made of the inherent Auger line shape.

More effort will need to be made by theorists and experimentalists if we are to understand and model the shake-up/shake-off processes in the Auger spectra of solids. Without a good physical model that enables the shake-up/shake-off function to be accurately determined for a given system, it will be difficult to achieve reliable qualitative and quantitative interpretation of Auger data.

#### IV. CONCLUSIONS

Auger photoelectron coincidence spectroscopy studies show the relative importance of the three- and four-hole

initial-state shake processes in the  $L_{23}VV$  spectra of  $3d$  transition metals. These can have a significant contribution to the low-energy tail of those spectra, and need to be accounted for in any qualitative or quantitative analysis using Auger spectroscopy.

#### ACKNOWLEDGMENTS

This work has been well supported by the Australian Research Council (ARC). Two of us (A.B.W. and C.P.L.) have been supported by an ARC funded position.

- 
- <sup>1</sup>G. D. Mahan, *Phys. Rev.* **163**, 612 (1967).  
<sup>2</sup>P. Nozieres and C. T. de Dominicis, *Phys. Rev.* **178**, 1097 (1969).  
<sup>3</sup>S. Doniach and M. Sunjic, *J. Phys. C* **3**, 285 (1970).  
<sup>4</sup>P. Steiner, H. Hochst, and S. Hufner, *Z. Phys. B* **30**, 129 (1978).  
<sup>5</sup>D. R. Penn, *Phys. Rev. Lett.* **40**, 568 (1978).  
<sup>6</sup>S. Tougaard, *Surf. Interf. Anal.* **11**, 453 (1978).  
<sup>7</sup>S. Tougaard and J. Kraaer, *Phys. Rev. B* **43**, 1651 (1991).  
<sup>8</sup>S. M. Thurgate, in *The Structure of Surfaces III*, edited by S. Y. Yong, M. A. van Hove, K. Takayanagi, and X. D. Xie (Springer-Verlag, Berlin, 1991), p. 179.  
<sup>9</sup>S. M. Thurgate, B. D. Todd, B. Lohmann, and A. Stelbovics, *Rev. Sci. Instrum.* **61**, 3733 (1990).  
<sup>10</sup>S. M. Thurgate, *Surf. Interf. Anal.* **20**, 627 (1993).  
<sup>11</sup>H. W. Haak, G. A. Sawatsky, and T. D. Thomas, *Phys. Rev. Lett.* **41**, 1825 (1978).  
<sup>12</sup>S. Tanuma, C. J. Powell, and D. R. Penn, *Surf. Interf. Anal.* **11**, 577 (1988).  
<sup>13</sup>D. Sarma, C. Carbone, P. Senn, R. Cimino, and W. Gudat, *Phys. Rev. Lett.* **63**, 656 (1989).  
<sup>14</sup>S. Whitfield, G. B. Armen, R. Car, J. C. Levin, and B. Crasemann, *Phys. Rev. A* **37**, 419 (1988).  
<sup>15</sup>N. Martensson, R. Nyholm, and B. Johansson, *Phys. Rev. B* **30**, 2245 (1984).  
<sup>16</sup>S. M. Thurgate and J. Neale, *Surf. Sci. Lett.* **256**, L605 (1991).  
<sup>17</sup>E. Jensen, R. A. Bartynski, R. F. Garrett, S. L. Hulbert, E. D. Johnson, and C.-C. Kao, *Phys. Rev. B* **45**, 13 636 (1992).  
<sup>18</sup>T. A. Carlson, *Photoelectron and Auger Spectroscopy* (Plenum, New York, 1974), p. 298.